Title

Differential metabolic and multi-tissue transcriptomic responses to fructose consumption among genetically diverse mice.

Journal

Biochimica et Biophysica Acta (BBA): Molecular Basis of Disease, 1866(1)

Authors

Zhang, Guanglin
Byun, Hyae
Ying, Zhe
et al.

Publication Date

2020

DOI

10.1016/j.bbadis.2019.165569

Peer reviewed

HHS Public Access

Author manuscript

Biochim Biophys Acta Mol Basis Dis. Author manuscript; available in PMC 2021 January 01.

Published in final edited form as:

Biochim Biophys Acta Mol Basis Dis. 2020 January 01; 1866(1): 165569. doi:10.1016/j.bbadis.2019.165569.

Differential Metabolic and Multi-tissue Transcriptomic Responses to Fructose Consumption among Genetically Diverse Mice

Guanglin Zhang[1], **Hyae Ran Byun**[1], **Zhe Ying**[1], **Montgomery Blencowe**[1], **Yuqi Zhao**[1], **Jason Hong**[1], **Le Shu**[1], **Karthick Chella Krishnan**[2], **Fernando Gomez-Pinilla**[1,3], **Xia Yang**[1,4,5]

[1]Department of Integrative Biology and Physiology, University of California, Los Angeles, Los Angeles, California 90095, USA

[2]Department of Medicine/Division of Cardiology and Department of Human Genetics, University of California, Los Angeles, Los Angeles, CA, USA

[3]Department of Neurosurgery, UCLA Brain Injury Research Center, University of California, Los Angeles, Los Angeles, California 90095, USA

[4]Institute for Quantitative and Computational Biosciences, University of California, Los Angeles, Los Angeles, California 90095, USA

[5]Molecular Biology Institute, University of California, Los Angeles, Los Angeles, California 90095, USA

Abstract

Understanding how individuals react differently to the same treatment is a major concern in precision medicine. Metabolic challenges such as the one posed by high fructose intake are important determinants of disease mechanisms. We embarked on studies to determine how fructose affects differential metabolic dysfunctions across genetically dissimilar mice, namely, C57BL/6J (B6), DBA/2J (DBA) and FVB/NJ (FVB), by integrating physiological and gene regulatory mechanisms. We report that fructose has strain-specific effects, involving tissue-specific

Correspondence: Xia Yang, Ph.D., Department of Integrative Biology and Physiology, University of California, Los Angeles, Los Angeles, CA 90095, USA, Phone: +1-310-206-1812, xyang123@ucla.edu, Fernando Gomez-Pinilla, Ph.D., Department of Neurosurgery and Department of Integrative Biology and Physiology, University of California, Los Angeles, Los Angeles, CA 90095, USA, Phone: +1-310-206-9693. fgomezpi@ucla.edu.

Author Contributions. G.Z., H.B., Z.Y., and K.C-K contributed to the experiments of the study. G.Z., J.H., X.Y. wrote the manuscript which was subsequently reviewed and revised by all the other authors. G.Z., M.B., Y.Z., L.S. performed the data analysis. X.Y., F. G-P. designed and supervised the study. X.Y. is the guarantor of this work and, as such, had full access to all the data in the study and takes responsibility for the integrity of the data and the accuracy of the data analysis.

Declaration of interests. No potential conflicts of interest relevant to this article were reported.

Data and Resource Availability. The datasets of RNAseq generated during the current study are available in Gene Expression Omnibus with series accession number GSE123896.

Declaration of interests

The authors declare that they have no known competing financial interests or personal relationships that could have appeared to influence the work reported in this paper.

gene regulatory cascades in hypothalamus, liver, and white adipose tissues. DBA mice showed the largest numbers of genes associated with adiposity, congruent with their highest susceptibility to adiposity gain and glucose intolerance across the three tissues. In contrast, B6 and FVB mainly exhibited cholesterol phenotypes, accompanying the largest number of adipose genes correlating with total cholesterol in B6, and liver genes correlating with LDL in FVB mice. Tissue-specific network modeling predicted strain-and tissue-specific regulators such as *Fgf21* (DBA) and *Lss* (B6), which were subsequently validated in primary hepatocytes. Strain-specific fructose-responsive genes revealed susceptibility for human diseases such that genes in liver and adipose tissue in DBA showed strong enrichment for human type 2 diabetes and obesity traits. Liver and adipose tissues genes in FVB were mostly related to lipid traits, and liver and adipose genes in B6 showed relevance to most cardiometabolic traits tested. Our results show that fructose induces gene regulatory pathways that are tissue specific and dependent on the genetic make-up, which may underlie interindividual variability in cardiometabolic responses to high fructose consumption.

Keywords

Fructose; Metabolic syndrome; Insulin resistance; Obesity; Personalized nutrition; Transcriptome

1. Introduction

One critical question in biomedical research is why individuals react differently to the same challenge or treatment such as metabolic perturbations through dietary modulation. Differential phenotypic responses to a metabolic perturbation across individuals can stem from differences in the host genome, epigenome, and their transcriptomic expression, which can shed light on the molecular mechanisms underlying inter-individual variability.

High fructose consumption is increasingly recognized as a risk factor for the escalating prevalence of metabolic syndrome (MetS) worldwide, posing significant risks for type 2 diabetes mellitus (T2D), obesity, cardiovascular diseases, and non-alcoholic fatty liver disease [1–5]. Previous evidence suggests that fructose affects obesity phenotypes differently between mouse strains [6], but inter-individual variability in the broader spectrum of cardiometabolic phenotypes such as glucose and lipid homeostasis as well as the molecular mechanisms underlying the variability remain unclear. To this end, we systematically examined the metabolic parameters and tissue-specific gene regulation in response to fructose consumption in genetically divergent inbred mouse strains, namely, C57BL/6J (B6), DBA/2J (DBA) and FVB/NJ (FVB) as they have broader genetic differences and demonstrate distinct physiological and pathological characteristics [6, 7].

To explore the molecular underpinnings of the variable responses to fructose, we focused on transcriptomic studies of the hypothalamus, liver, and adipose tissues based on their critical roles in metabolic regulation. The hypothalamus is a master regulator of nutrient sensing, food intake, energy expenditure, body weight, and glucose metabolism [8, 9], and is sensitive to fructose consumption [10]. The liver is a main regulator of glucose, fructose, steroid, and lipid metabolism [11]. White adipose tissue (WAT) is essential for energy and

lipid storage, hormone secretion, and inflammation involved in MetS [12, 13]. Here we report that fructose has differential effects on the gene regulatory cascades of these tissues among mice of divergent genetic makeup and offer insights into key genes and pathways underlying the individualized metabolic perturbations carried by fructose. Lastly, integration of the strain- and tissue-specific genes affected by fructose with human disease susceptibility profiles from genome-wide association studies (GWAS) indicates that the fructose-induced gene network perturbations are relevant to cardiometabolic risks in humans.

2. Methods

2.1 Animals

Male DBA, B6 and FVB mice (Jackson Laboratory, Bar Harbor, ME) of 8-week age weighing 20–25g were randomly assigned to 8% w/v fructose in drinking water (n=8–12/strain) and control group (n=8–10/strain, drinking water) for 12 weeks. We chose 8% fructose in drinking water to mimic the intake route and the average fructose consumption found in sugar-sweetened beverages (~10% w/v) consumed in humans. All mice had free access to water and a standard Chow diet (Lab Rodent Diet 5001, LabDiet, St Louis, MO) and were maintained under standard housing condition (22–24°C) with 12h light/dark cycle. Daily food and drink intake were monitored on per-cage basis. Each mouse was examined for changes in a wide spectrum of metabolic phenotypes including body weight, fat mass, lean mass, intraperitoneal glucose tolerance test (IPGTT), and plasma levels of insulin, glucose, and lipids. Mice were sacrificed at the end of the fructose treatment (12-week), and hypothalamus, liver, and various WAT depots (mesenteric [mWAT], subcutaneous [scWAT], gonadal [gWAT], and intraperitoneal [iWAT]) were dissected out, weighed, flash frozen and stored at −70°C.

2.2 Body weight and body mass composition

Body weight was measured weekly and body mass composition (lean mass, fat mass) was determined by NMR in a Bruker minispec series mq10 machine (Bruker BioSpin, Freemont, CA) every two weeks.

2.3 IPGTT

Prior to IPGTT at the 1st, 4th, 9th and 12th week of fructose treatment, the animals were fasted overnight at each time point. Each mouse was injected intraperitoneally with 20% glucose at 2g glucose/kg body weight. Blood glucose levels from tail vein were measured at 0, 15, 30, 90, and 120 min after glucose injection using an AlphaTrak blood glucose meter (Abbott Laboratories, North Chicago, IL). Area under the curve (AUC) was calculated as a measure of glucose tolerance.

2.4 Plasma lipids and glycemic traits

Mice were fasted overnight before sacrifice, and blood samples were collected through retro-orbital bleeding. Plasma total cholesterol (TC), high density lipoprotein cholesterol (HDL), unesterified cholesterol (UC), free fatty acids (FFA), triglycerides (TG), glucose, and insulin were measured by enzymatic colorimetric assays at UCLA GTM Mouse Transfer Core as

previously described [10]. Low density lipoprotein cholesterol (LDL) was calculated as LDL = TC - HDL - (TG/5).

2.5 RNA sequencing (RNAseq) and data analysis

Total RNA was extracted from hypothalamus, liver, and mWAT tissues (n=6/tissue/group/strain for liver and mWAT; n=4/group/strain for hypothalamus) using All-Prep DNA/RNA/miRNA Universal Kit (Qiagen, CA. USA). mWAT was chosen due to its stronger implications in MetS than other fat depots [14]. Sample size was based on previous RNAseq studies in which findings were validated using qPCR and gene perturbation experiments [10, 15, 16]. RNA quality was evaluated, and libraries were prepared for samples passing quality control and sequenced in pair-end mode on an Illumina HiSeq 4000 sequencer as previously described [10, 15, 16]. We employed a pipeline containing HISAT, StringTie and Ballgown [17] to align reads to mouse genome mm10 [18], assemble transcripts [19], and identify differentially expressed genes (DEGs) using a linear model test after filtering genes with low expression levels (FPKM<1) [20]. Multiple testing was corrected using the q value approach and false discovery rate (FDR) < 0.05 was used to determine significant DEGs. DEGs were assessed for enrichment of pathways in Gene Ontology and KEGG using the DAVID tool [21, 22]. Pathways at FDR <0.05 were considered significant.

2.6 Identification of network key drivers (KDs) of fructose DEGs

Our previously constructed Bayesian networks of hypothalamus, liver, and adipose tissues were used to investigate the gene-gene regulations among the fructose DEGs and to identify potential regulators (details in Supplemental Materials) [23, 24]. The weighted key driver analysis (wKDA) in Mergeomics [25] was employed to predict key regulatory genes, or KDs, of the fructose DEGs from each tissue and each strain. KDs are defined as the network genes whose network neighboring genes were significantly enriched for fructose DEGs based on a Chi-square like statistics followed by FDR assessment in wKDA [25]. Network genes reaching FDR < 0.05 were reported as potential KDs. The gene subnetworks of KDs were visualized using Cytoscape [26].

2.7 Validation of strain-specificity and regulatory role of predicted liver KDs

Primary hepatocytes were isolated from male B6 (n=3) and DBA mice (n=3) of 12 weeks of age. Mouse was perfused at a rate of 4.5 ml/minute through port vein with perfusion medium (GIBCO 17701–038, Thermo Fisher Scientific, CA, USA) for 5 minutes followed by digestion medium (GIBCO 17703–034, Thermo Fisher Scientific, CA, USA) for 7 minutes. The liver was torn into pieces, filtered and pelleted down at 50g for 3 minutes at 4°C, followed by the addition of 20 ml 40% cold Percoll and centrifugation at 200g for 7 minutes at 4°C to separate live and dead hepatocytes. After washing twice, hepatocytes were seeded in collagen coated plate at $2.2*10e^5$ cells/6-well. Medium was changed after 4-hour incubation at 37°C with 5% CO_2. Primary hepatocytes were subject to fructose treatment at 5mM and 45mM concentrations for 6, 12, 24 and 48 hours. We then isolated RNA and analyzed expression levels of *Fgf21* and *Lss* using qPCR (Supplementary Table 1). β-actin was used as internal control for qPCR, while *Gapdh* was found to show variable response to fructose and therefore was not used as internal control.

To validate the role of these predicted KDs in regulating gene subnetworks, we used siRNAs (Sigma-Aldrich, St. Louis, MO; Supplementary Table 1) to knockdown *Fgf21* or *Lss*. siRNAs were delivered into cells using Lipofectamine RNAiMAX (Invitrogen, CA). Six oligos for *Fgf21* and three oligos for *Lss* were tested, among which one for *Fgf21* and two for *Lss* achieved >60% knockdown efficiency and were used for knockdown experiments (Supplementary Figure 1). The expression changes in ten predicted downstream network genes as well as five negative control genes not in the relevant networks were evaluated using qPCR (Supplementary Table 1). *Gapdh* was used as internal control for qPCR as it showed stable expression. Differential gene expression in each subnetwork gene was evaluated using two-sided Student's t-test. For *Lss*, data from the two oligos were pooled for statistical analysis.

2.8 Correlation between fructose DEGs and phenotypic characteristics

To assess whether and which of the fructose DEGs were related to the metabolic phenotypes, we calculated the Pearson correlation between the DEGs and individual metabolic traits. Benjamini-Hochberg was used to control FDR.

2.9 Relevance of the fructose DEGs to human GWAS genes of cardiometabolic diseases

Summary statistics of human GWAS for ten metabolic phenotypes related to obesity, T2D, and coronary artery disease (CAD) were retrieved from GWAS catalog [27] (Supplementary Table 2). The fructose DEGs from our mouse study were assessed for enrichment of human GWAS signals using the marker set enrichment analysis (MSEA) in Mergeomics [25]. DEGs from each tissue and strain were first mapped to tissue-matched expression SNPs (eSNPs) at the Mergeomics web server [25]; eSNPs in high linkage disequilibrium of $r^2 > 0.7$ were filtered out. For each GWAS, the trait/disease association p-values of the eSNPs of each DEG list were compared to those of random genes of matching size using a Chi-square like statistics [25] to determine the significance of association between the DEGs and diseases. MSEA enrichment p values were adjusted using Bonferroni-correction for 9 DEG sets x 10 GWAS sets.

2.10 Statistics

For metabolic phenotypes, two-sided Student's t test was used to determine statistical differences between fructose-fed and control mice within each mouse strain. For phenotypes measured at multiple time points, two-way ANOVA were used to determine the significance of fructose treatment and time points. The statistics of genomic analyses was described in the corresponding sections above. Data are expressed as mean ± SEM.

2.11 Study approval

This study was performed in accordance with National Institutes of Health Guide for the Care and Use of Laboratory Animals. The experimental protocol was approved by the Chancellor's Animal Research Committee of the University of California at Los Angeles.

3. Results

3.1 Distinct metabolic responses to fructose consumption between mouse strains

In response to 12-week fructose consumption, fructose-fed DBA mice gained significant body weight, fat mass, and percent fat mass compared to the water group, while B6 and FVB showed no differences (Fig. 1A–F). In addition, only fructose-fed DBA mice showed a significant decrease in percent lean mass (Fig. 1H) but not lean mass (Fig. 1G), along with significant increases in the weights of rWAT, mWAT, and scWAT (Fig. 1I) at the end of the 12-week fructose treatment. The decrease in percent lean mass could be driven by increases in fat mass but not lean mass itself. Total caloric intake was similar between treatment groups (Fig. 1J), with an increasing trend for fructose intake accompanied by a decrease in food intake across strains (Supplementary Fig. 2). The body composition differences were also not explained by the amount of fructose intake, as B6 (resistant) and DBA (susceptible) had similar fructose intake whereas FVB (resistant) had higher fructose intake (Supplementary Fig. 2).

Fructose consumption caused increased glucose AUC in DBA mice starting at the 4^{th} week till the 12^{th} week, indicating that fructose impaired glucose homeostasis in DBA. In contrast, B6 and FVB exhibited no difference between treatment groups (Fig. 2A–C). No significant difference in plasma glucose levels was observed between treatment groups for any of the strains (Fig. 2D), but DBA and FVB showed significantly elevated plasma insulin levels in fructose-fed mice (Fig. 2E).

In contrast to the stronger obesity and diabetic phenotypes in fructose-fed DBA mice, lipid traits did not change in DBA. Fructose-fed B6 mice had increased levels of TC, UC, HDL and LDL, while fructose-fed FVB mice displayed elevated TG and FFA but reduced TC, UC, and LDL (Fig. 2F–K).

3.2 Distinct transcriptomic changes in response to fructose in metabolic tissues of different mouse strains

To explore the potential mechanisms underlying the differences in metabolic phenotypes among the mouse strains, we examined the transcriptomic alterations in tissues relevant to nutrient sensing, energy homeostasis, and metabolic regulation. RNAseq of tissues from B6, DBA and FVB mice identified 578, 760 and 246 DEGs in liver, 484, 119 and 25 DEGs in hypothalamus, and 1034, 884, and 427 DEGs in the adipose tissues, respectively, at a threshold of FDR < 0.05 (Fig. 3A–C; top DEGs in Table 1; full DEGs in Supplementary Table 3). Based on the DEG numbers, DBA liver and adipose tissues and all three tissues from B6 appear to be more sensitive to fructose compared to FVB.

Comparison of the DEGs within each tissue across mouse strains revealed high strain-specificity (Fig. 3A–C). Only four adipose DEGs, 15 liver DEGs, and one hypothalamus DEG overlapped across strains (Fig. 3A–C). Among these, only three genes (*Jun* from adipose tissue, *Id3* from liver, and *Cd200* from hypothalamus) showed consistent direction of changes across strains (Supplementary Table 3).

Previous studies have revealed ChREBP and SREBP-1c as transcription factors that regulate fructose activities in the liver [28–30]. We examined the expression of ChREBP (gene *Mlxipl*), SREBP-1c (gene *Srebf1*), and their known target genes in our liver transcriptome data. *Mlxip1* was significantly altered only in DBA while no changes in *Srebf1* were found in any of the strains. However, many of their target genes such as *Aldob*, *Dgat1*, *Dgat2*, *Fgf21* and *Gck* were significantly altered by fructose in the liver, particularly in DBA mice (Fig. 3D). Of the genes involved in fructose metabolism [29, 31], *Khk* was downregulated in B6 while upregulated in DBA and FVB, and *Aldob* was downregulated in DBA (Fig. 3D).

3.3 Functional categorization of fructose DEGs reveals alterations of strain- and tissue-specific pathways

We annotated the functions of the DEGs and identified tissue- and strain-specific biological pathways affected by fructose (top pathways in Table 1; full results in Supplementary Table 4). Within adipose tissue, B6 DEGs were mainly related to oxidation pathways; DBA DEGs were enriched for nucleosome assembly genes; protein folding/processing pathways were enriched in FVB DEGs. For liver, B6 DEGs were over-represented with oxidation, lipid and cholesterol metabolic pathways; DBA DEGs were related to oxidation, PPAR signaling, and fatty acid, lipid and cholesterol metabolic pathways; FVB DEGs were enriched for genes involved in vesicle mediated transport. For the hypothalamus, B6 DEGs were involved in oxidative phosphorylation and protein translation while DBA DEGs were related to protein processing.

3.4 wKDA analysis prioritized strain- and tissue-specific key drivers (KDs) of fructose DEGs

To explore the potential regulatory genes upstream of the fructose-induced DEGs, we used a data-driven network analysis, wKDA, to pinpoint key regulatory genes of fructose activities in individual tissues/strains. This type of analysis previously identified novel regulators of various diseases which were subsequently validated via gene perturbation experiments [10, 32–34]. Using wKDA, we predicted KDs of the fructose DEGs from each tissue/strain using tissue-specific gene regulatory networks (top KDs in Table 1; full lists in Supplementary Table 5). As shown in Fig. 4A–C, the top KDs in each tissue orchestrate numerous strain-specific DEGs and there were distinct subnetworks highlighting unique organization of DEGs from each strain.

In liver, the top KDs for B6 DEGs were mostly related to sterol/cholesterol biosynthesis such as *Dhcr7, Fdft1,* and *Lss*. The top KDs for DBA included *Fgf21*, a target of ChREBP and a metabolic regulator for insulin sensitivity and obesity [6, 35], *Insig2*, a negative regulator of SREBP targeting lipid metabolism [36], *Irgm*, which induces inflammatory cytokine production [37], and *Arntl*, a key circadian rhythm gene. FVB top liver KDs included *Itih3*, implicated in liver glutathione metabolism [38], and *Akr1d1*, important for bile acid and steroid hormone metabolism [39].

For adipose tissue, DBA-specific KDs are involved in inflammation (*Cd68*, *Itgis*), obesity (*Dio2*), and cell cycle (*Evi2b*, *Ptpn18*); B6-specific KDs are related to branched chain amino acid (BCAA) metabolism (*Aldh6a1, Echs1, Hadh, Hibadh, Hibch*); FVB KDs are related to

kynurenine pathway which is activated in obesity [40] (*Ccbl2*) and BCAA metabolism (*Hibch*, *Cpa1*). For hypothalamus, KDs were identified only for the B6 DEGs, and many were extracellular matrix genes (e.g., *Fmod, Foxc2, Bgn*).

3.5 Experimental validation of strain- and tissue-specific KDs

The B6-specific hypothalamic KDs *Fmod* and *Bgn* were previously found to be hypothalamic KDs in a rat fructose study [10]. Ablation of *Fmod* or *Bgn* in mice led to altered metabolic phenotypes and tissue-specific pathways that overlap with those affected by fructose [10, 41].

To validate additional strain-specific KDs, we prioritized *Fgf21* and *Lss* based on several criteria. First of all, we focused on the predicted top key drivers in Table 1, and *Fgf21* and *Lss* were both among the top predicted regulatory genes. Secondly, we visualized the gene networks derived from the key driver analysis to identify distinct key driver subnetworks of each mouse strain (Figure 4). We found that *Fgf21* was mostly surrounded by DBA DEGs whereas *Lss* had mostly B6 DEGs as network neighbors, supporting their strong strain-specificity. Thirdly, we focused on liver network since liver is a main organ metabolizing fructose, and both genes were predicted liver regulators. Lastly, among the top strain-specific liver key drivers, *Fgf21* has been linked to obesity, and *Lss* is involved in cholesterol metabolism, which agreed with the phenotypic changes in DBA and B6, respectively. We tested the B6-specific liver KD *Lss* and the DBA-specific liver KD *Fgf21* by treating primary hepatocytes isolated from B6 and DBA with fructose. Agreeing with the strain specificity of the KD predictions based on our liver transcriptome data, *Fgf21* was particularly responsive to fructose in DBA hepatocytes (Fig. 4D) and *Lss* was more responsive to fructose in B6 hepatocytes (Fig. 4E). Perturbing these predicted KDs using siRNAs also affected liver network genes (selected from Fig. 4B) surrounding the respective KDs (Fig. 4F–G). As negative controls, we selected five genes from fructose DEGs that were not shown in the *Fgf21/Lss* centered gene networks and examined their gene expression changes. These genes did not change significantly after *Lss/Fgf21* knockdown (Fig. 4H). Altogether, these results support the importance of the network analysis in predicting functional aspects of gene regulation in response to fructose.

3.6 Relationship between DEGs and metabolic phenotypes in mouse and human

To investigate the relationships between fructose DEGs and cardiometabolic phenotypes, we performed a correlation analysis to identify DEGs that show correlation with individual phenotypes in the three mouse strains. At an unadjusted $P < 0.01$, DBA had the largest numbers of adiposity-correlated DEGs from each of the three tissues (Fig. 5A; Supplementary Table 6). In contrast, B6 had the largest number of adipose DEGs correlating with TC, and FVB liver DEGs showed correlations with LDL, which are consistent with the observed cholesterol phenotypes in these strains. Few of the hypothalamic DEGs correlated with the metabolic phenotypes measured. At FDR < 0.05, DBA liver DEGs involved in lipid metabolism and adipogenesis (*St6gal1*, *Scd1*, and *Pla2g6*) were correlated with adiposity (Fig. 5B–D) and FVB liver DEGs (*Aldh2, Enho, Svip*) were correlated with LDL (Fig. 5E–G).

To assess the association between the fructose DEGs with human cardiometabolic disorders, we performed GWAS enrichment analysis using Mergeomics [42]. As shown in Table 2, DBA liver and adipose DEGs showed strong enrichment for human GWAS signals for T2D and obesity traits; FVB DEGs from liver and adipose tissues are mostly related to lipid traits; B6 liver and adipose DEGs showed relevance to most cardiometabolic traits tested. For example, a SNP of a B6 liver DEG *FADS2,* was associated with lipid profiles in two Asian groups [43]. Polymorphisms of *LIPC*, a gene altered by fructose in DBA liver, have been associated with obesity and overweight in humans [44, 45] (Supplementary Table 7). These results suggest that the fructose-affected genes identified from the various mouse strains are relevant to different aspects of human cardiometabolic diseases.

4. Discussion

Our multi-strain, multi-tissue, multi-phenotype systems analysis shows that fructose consumption elicits differential phenotypic and transcriptomic profiles among mice of different genetic background. At the phenotypic level, DBA mice exhibited stronger vulnerability to alterations in body composition and glucose intolerance while B6 and FVB mice had stronger cholesterol alterations. We also report strain-specific regulatory genes and pathways in key metabolic tissues that may underlie the inter-individual differential responses to fructose. Gene-phenotype correlation analysis and human GWAS enrichment analysis suggest that the fructose-affected genes are relevant to cardiometabolic phenotypes in both mouse and human.

Our findings are in line with previous studies that demonstrated personalized responses to diets [6, 7, 46] and offer a comprehensive account of the fructose-induced metabolic and molecular differences between genetically dissimilar mouse strains. Interestingly, the patterns of phenotypic differences are not only strain-specific but also diet-specific. For example, among the three strains (B6, DBA, and FVB), B6 mice gained the most weight when fed a high fat high sucrose diet [7] but had little weight or adiposity change when on high fructose, whereas DBA mice gained the most weight when fed a fructose diet and were relatively resistant to the high fat high sucrose diet. This diet-specific variability across strains indicates different adaptive abilities of distinct genetic background towards different diets.

Our transcriptomic studies provide clues to the potential molecular underpinnings of the differential metabolic responses to fructose between mouse strains. In particular, we found very limited overlap between strains in the DEGs altered by fructose in individual tissues, and unique pathways represented by the strain-specific DEGs are biologically relevant to the distinct phenotypes in the corresponding mouse strains, as detailed below.

Liver-specific DEGs in the DBA mice were uniquely enriched for the PPAR signaling pathway, which agrees with results that DBA was the only strain to gain weight and fat mass and to show glucose intolerance in response to fructose. Additionally, our network modeling revealed *Fgf21* to be a DBA-specific liver key regulator of fructose response. FGF21 is a hormone primarily produced in the liver and holds promise as a potential therapy for obesity and glucose intolerance [47, 48]. We found chronic consumption of fructose inhibits *Fgf21*

in DBA mice, which agrees with their compromised glucose homeostasis and increased adiposity. Our *in vitro* fructose treatment experiments in primary hepatocytes confirmed that *Fgf21* is a direct and acute target of fructose, particularly in DBA. There is also an interesting directional shift in *Fgf21* between the acute fructose response in primary hepatocytes where *Fgf21* immediately increases upon fructose treatment at early time points, whereas in our long-term (12-week) *in vivo* study *Fgf21* is inhibited by fructose most significantly in DBA. Perhaps *Fgf21* is an early homeostatic regulator in DBA mice with a quick response to fructose upon initial exposure, but after chronic exposure, fructose or its metabolites or other downstream effectors inhibit *Fgf21*. Further measurement of circulating FGF21 in our limited remaining plasma samples (n=4–6 samples/group) showed a decreasing trend consistent with the mRNA level changes observed in DBA (Supplementary Figure 3). Future larger experiments are needed to further explore the role of circulating FGF21 in fructose response in DBA.

In contrast, B6 liver DEGs and top KDs are primarily cholesterol related genes, agreeing with the cholesterol-centric phenotypic responses of B6 to fructose. In FVB mice, DEGs, their predicted KDs, and the phenotype-correlated genes are related to vesicle mediated transport, protein processing, and metabolic pathways involving glutathione, cytochrome P450, and lipids. These may play roles in the unique decrease in plasma cholesterol and LDL levels in response to fructose in this strain.

In the hypothalamus, fructose induced the strongest transcriptomic changes in B6 mice compared to the other two strains, and our network analysis revealed extracellular matrix genes such as *Fmod* and *Bgn* as key drivers of the fructose-responsive DEGs in B6 mice. This is consistent with our previous rat study in which these genes were also identified as key regulators in the hypothalamus in response to fructose consumption [10]. Both *Fmod* and *Bgn* knockout mice showed significantly altered cholesterol phenotypes [10], agreeing with the significant increases in these traits in B6 in response to fructose. Additional studies of *Bgn* knockout mice also confirmed the essential role of *Bgn* in mediating the fructose effects and in regulating brain and peripheral gene networks [41]. Besides the hypothalamic regulators, the B6-specific increases in cholesterol species in response to fructose could also be related to dysregulation of liver key drivers related to cholesterol biosynthesis such as *Lss* as revealed in our network analysis. *Lss* encodes lanosterol synthase which converts (S)-2,3 oxidosqualene to lanosterol, a key intermediate in cholesterol biosynthesis, and there is growing interest in targeting this enzyme therapeutically to lower blood cholesterol [49]

Upon examining previously known gene regulatory mechanisms involving transcription factors ChREBP and SREBP-1c in the liver [28–30], we found indirect evidence supporting their regulatory roles by observing changes in their target genes. Fructose metabolic enzymes such as *Khk* and *Aldob* also showed alterations but the direction of change and significance varied between strains in our 12-week fructose feeding study. In addition to these known factors regulating fructose activities, our data-driven network analysis revealed numerous strain-specific regulators in individual tissues, such as *Fgf21* (DBA), *Lss* (B6), and *Akr1d1* (FVB) in liver, BCAA genes (B6 and FVB) and *Dio2* (DBA) in adipose tissue, and extracellular matrix genes *Bgn* and *Fmod* (B6) in hypothalamus. These context-specific regulatory genes identified here extend our knowledge about how fructose perturbs divergent

pathways and triggers differential metabolic manifestations between individuals. Further investigations of these regulators, the genetic determinants of their context-dependent interactions with fructose or metabolites, and their downstream gene networks/pathways are warranted.

In addition to the strain-specific DEGs and regulators, our transcriptomic analysis also revealed certain shared fructose DEGs across strains, including those involved in the response to xenobiotic stimulus (*Gstp1, Ephx1, Gstm1*) or organic cyclic compounds (*Abca1, Id3, Abat*), metabolic processes (*Abca1*, *Htatip2*, *Grhpr*, *Nudt7*), transcriptional regulation (*Ier5*, *Jun*, *Id3*), and immune modulation (*Cd200*). These represent robust targets of fructose regardless of genetic background and may be exploited to counteract the effects of fructose in the general population.

As evidence supporting the roles of the DEGs in cardiometabolic disorders, we found strain-specific DEGs to be correlated with specific phenotypes in the three mouse strains, e.g., DBA had the largest number of adiposity-correlated DEGs from each of the three tissues. Furthermore, our GWAS enrichment analysis also connected the fructose-affected genes to human cardiometabolic diseases [42]. Although in each of the tissues and strains, fructose perturbed different sets of genes and pathways, they all point to various aspects of cardiometabolic disorders. These results are important in the context of abundant public health and anecdotal information regarding differential responses to fructose and other dietary factors across individuals.

Overall, our findings from three different mouse models showed consistencies as well as differences compared to previous human and rat studies. The increased adiposity and lipogenic responses in fructose-fed mice as well as the perturbations in adipogenic and lipid pathways observed in our mouse studies are supported by the obesogenic and lipogenic effects observed in human epidemiology studies [2, 4, 5, 50]. In addition, human epidemiological studies also support the connection between fructose consumption and glycemic and insulin responses observed in DBA mice in our study [4, 51, 52]. The glycemic phenotypes observed in our mouse study appeared to be modest compared to previous rat studies. One of the potential reasons could be the much lower fructose dose used in this study (8% to better mimic human exposure level) compared to most rat studies (15% fructose or higher). The difference in dosage makes it difficult to concretely state whether mice are more resistant than rats. However, there is evidence supporting that mice might have better capacity to metabolize fructose than rats and humans [53], which likely leads to more resistance to fructose effects in mice. We speculate that different mouse strains also differ in their ability to metabolize or clear fructose, which may partially underlie the differential responses to fructose between strains. For instance, compared to the other two mouse strains examined, FVB mice had significantly increased fructose consumption but had minimal metabolic and transcriptomic changes. It is possible that FVB has stronger ability to metabolize or clear fructose than the other strains, which warrants further investigation.

At the transcriptome level, compared to previous human studies of skeletal muscle transcriptome of first-degree relatives of diabetic patients with 6 or 7-day fructose

consumption [54, 55], perturbations in oxidation, lipid and fatty acid metabolism pathways were consistently observed in our mouse studies, although numerous additional tissue-specific pathways were also revealed in our studies. We have previously conducted a rat study on the effect of fructose on brain transcriptome focusing on the hypothalamus and hippocampus. The hypothalamic DEGs of B6 and FVB mice showed significant overlap with the rat hypothalamic DEGs, and pathways related to TGF-beta signaling, axon guidance, extracellular matrix organization, and insulin/IGF signaling were shared. The top hypothalamic key drivers such as *Fmod* and *Bgn* were also consistent. However, no significant overlap was found between the DBA DEGs and the rat DEGs. These results suggest certain shared biological responses as well as differences between species.

It is important to note that our study employed overnight fasting to reduce variability in the lipids and glycemic measurements. However, overnight fasting induces significant weight loss and nutrient changes, which could affect gene programs [56–58] and mask certain fructose-responsive pathways. Future studies examining shorter fasting duration, fed state, and fasted/refed state are necessary to further elucidate the gene regulatory targets of fructose.

In conclusion, we found distinct metabolic phenotypes and molecular signatures in mice of different genetic background in response to fructose. These results provide important insight into how individuals differ in their response to fructose consumption by engaging specific gene regulatory mechanisms in both central and peripheral metabolic tissues. Future examination of additional mouse strains, tissues, and fasting/fed conditions will help further dissect the inter-individual variability and tissue-specific genetic regulation of fructose response.

Supplementary Material

Refer to Web version on PubMed Central for supplementary material.

Acknowledgments

Funding. X.Y. and F.G-P. are funded by R01 DK104363, R01 NS50465 and R21 NS103088.

References

[1]. Lakka HM, Laaksonen DE, Lakka TA, Niskanen LK, Kumpusalo E, Tuomilehto J, Salonen JT, The metabolic syndrome and total and cardiovascular disease mortality in middle-aged men, JAMA, 288 (2002) 2709–2716. [PubMed: 12460094]

[2]. Te Morenga L, Mallard S, Mann J, Dietary sugars and body weight: systematic review and meta-analyses of randomised controlled trials and cohort studies, BMJ, 346 (2012) e7492. [PubMed: 23321486]

[3]. Yang Q, Zhang Z, Gregg EW, Flanders WD, Merritt R, Hu FB, Added sugar intake and cardiovascular diseases mortality among US adults, JAMA INTERN MED, 174 (2014) 516–524. [PubMed: 24493081]

[4]. Stanhope KL, Schwarz JM, Keim NL, Griffen SC, Bremer AA, Graham JL, Hatcher B, Cox CL, Dyachenko A, Zhang W, McGahan JP, Seibert A, Krauss RM, Chiu S, Schaefer EJ, Ai M, Otokozawa S, Nakajima K, Nakano T, Beysen C, Hellerstein MK, Berglund L, Havel PJ, Consuming fructose-sweetened, not glucose-sweetened, beverages increases visceral adiposity

and lipids and decreases insulin sensitivity in overweight/obese humans, J CLIN INVEST, 119 (2009) 1322–1334. [PubMed: 19381015]

[5]. Malik VS, Popkin BM, Bray GA, Despres JP, Willett WC, Hu FB, Sugar-sweetened beverages and risk of metabolic syndrome and type 2 diabetes: a meta-analysis, DIABETES CARE, 33 (2010) 2477–2483. [PubMed: 20693348]

[6]. Glendinning JI, Breinager L, Kyrillou E, Lacuna K, Rocha R, Sclafani A, Differential effects of sucrose and fructose on dietary obesity in four mouse strains, PHYSIOL BEHAV, 101 (2010) 331–343. [PubMed: 20600198]

[7]. Parks BW, Nam E, Org E, Kostem E, Norheim F, Hui ST, Pan C, Civelek M, Rau CD, Bennett BJ, Mehrabian M, Ursell LK, He A, Castellani LW, Zinker B, Kirby M, Drake TA, Drevon CA, Knight R, Gargalovic P, Kirchgessner T, Eskin E, Lusis AJ, Genetic control of obesity and gut microbiota composition in response to high-fat, high-sucrose diet in mice, CELL METAB, 17 (2013) 141–152. [PubMed: 23312289]

[8]. Morton GJ, Cummings DE, Baskin DG, Barsh GS, Schwartz MW, Central nervous system control of food intake and body weight, NATURE, 443 (2006) 289–295. [PubMed: 16988703]

[9]. Coll AP, Farooqi IS, O'Rahilly S, The hormonal control of food intake, CELL, 129 (2007) 251–262. [PubMed: 17448988]

[10]. Meng Q, Ying Z, Noble E, Zhao Y, Agrawal R, Mikhail A, Zhuang Y, Tyagi E, Zhang Q, Lee JH, Morselli M, Orozco L, Guo W, Kilts TM, Zhu J, Zhang B, Pellegrini M, Xiao X, Young MF, Gomez-Pinilla F, Yang X, Systems Nutrigenomics Reveals Brain Gene Networks Linking Metabolic and Brain Disorders, EBioMedicine, 7 (2016) 157–166. [PubMed: 27322469]

[11]. Rui L, Energy metabolism in the liver, COMPR PHYSIOL, 4 (2014) 177–197. [PubMed: 24692138]

[12]. Choe SS, Huh JY, Hwang IJ, Kim JI, Kim JB, Adipose Tissue Remodeling: Its Role in Energy Metabolism and Metabolic Disorders, Front Endocrinol (Lausanne), 7 (2016) 30. [PubMed: 27148161]

[13]. Coelho M, Oliveira T, Fernandes R, Biochemistry of adipose tissue: an endocrine organ, ARCH MED SCI, 9 (2013) 191–200. [PubMed: 23671428]

[14]. Bjorndal B, Burri L, Staalesen V, Skorve J, Berge RK, Different adipose depots: their role in the development of metabolic syndrome and mitochondrial response to hypolipidemic agents, J Obes, 2011 (2011) 490650. [PubMed: 21403826]

[15]. Meng Q, Zhuang Y, Ying Z, Agrawal R, Yang X, Gomez-Pinilla F, Traumatic Brain Injury Induces Genome-Wide Transcriptomic, Methylomic, and Network Perturbations in Brain and Blood Predicting Neurological Disorders, EBioMedicine, 16 (2017) 184–194. [PubMed: 28174132]

[16]. Shu L, Meng Q, Diamante G, Tsai B, Chen YW, Mikhail A, Luk H, Ritz B, Allard P, Yang X, Prenatal Bisphenol A Exposure in Mice Induces Multitissue Multiomics Disruptions Linking to Cardiometabolic Disorders, ENDOCRINOLOGY, 160 (2019) 409–429. [PubMed: 30566610]

[17]. Pertea M, Kim D, Pertea GM, Leek JT, Salzberg SL, Transcript-level expression analysis of RNA-seq experiments with HISAT, StringTie and Ballgown, NAT PROTOC, 11 (2016) 1650–1667. [PubMed: 27560171]

[18]. Kim D, Langmead B, Salzberg SL, HISAT: a fast spliced aligner with low memory requirements, NAT METHODS, 12 (2015) 357–360. [PubMed: 25751142]

[19]. Pertea M, Pertea GM, Antonescu CM, Chang TC, Mendell JT, Salzberg SL, StringTie enables improved reconstruction of a transcriptome from RNA-seq reads, NAT BIOTECHNOL, 33 (2015) 290–295. [PubMed: 25690850]

[20]. Frazee AC, Pertea G, Jaffe AE, Langmead B, Salzberg SL, Leek JT, Ballgown bridges the gap between transcriptome assembly and expression analysis, NAT BIOTECHNOL, 33 (2015) 243–246. [PubMed: 25748911]

[21]. Huang da W, Sherman BT, Lempicki RA, Systematic and integrative analysis of large gene lists using DAVID bioinformatics resources, NAT PROTOC, 4 (2009) 44–57. [PubMed: 19131956]

[22]. Huang da W, Sherman BT, Lempicki RA, Bioinformatics enrichment tools: paths toward the comprehensive functional analysis of large gene lists, NUCLEIC ACIDS RES, 37 (2009) 1–13. [PubMed: 19033363]

[23]. Zhu J, Wiener MC, Zhang C, Fridman A, Minch E, Lum PY, Sachs JR, Schadt EE, Increasing the power to detect causal associations by combining genotypic and expression data in segregating populations, PLOS COMPUT BIOL, 3 (2007) e69. [PubMed: 17432931]

[24]. Zhu J, Zhang B, Smith EN, Drees B, Brem RB, Kruglyak L, Bumgarner RE, Schadt EE, Integrating large-scale functional genomic data to dissect the complexity of yeast regulatory networks, NAT GENET, 40 (2008) 854–861. [PubMed: 18552845]

[25]. Arneson D, Bhattacharya A, Shu L, Makinen VP, Yang X, Mergeomics: a web server for identifying pathological pathways, networks, and key regulators via multidimensional data integration, BMC GENOMICS, 17 (2016) 722. [PubMed: 27612452]

[26]. Shannon P, Markiel A, Ozier O, Baliga NS, Wang JT, Ramage D, Amin N, Schwikowski B, Ideker T, Cytoscape: a software environment for integrated models of biomolecular interaction networks, GENOME RES, 13 (2003) 2498–2504. [PubMed: 14597658]

[27]. Buniello A, MacArthur JAL, Cerezo M, Harris LW, Hayhurst J, Malangone C, McMahon A, Morales J, Mountjoy E, Sollis E, Suveges D, Vrousgou O, Whetzel PL, Amode R, Guillen JA, Riat HS, Trevanion SJ, Hall P, Junkins H, Flicek P, Burdett T, Hindorff LA, Cunningham F, Parkinson H, The NHGRI-EBI GWAS Catalog of published genome-wide association studies, targeted arrays and summary statistics 2019, NUCLEIC ACIDS RES, 47 (2019) D1005–D1012. [PubMed: 30445434]

[28]. Kim MS, Krawczyk SA, Doridot L, Fowler AJ, Wang JX, Trauger SA, Noh HL, Kang HJ, Meissen JK, Blatnik M, Kim JK, Lai M, Herman MA, ChREBP regulates fructose-induced glucose production independently of insulin signaling, J CLIN INVEST, 126 (2016) 4372–4386. [PubMed: 27669460]

[29]. Herman MA, Samuel VT, The Sweet Path to Metabolic Demise: Fructose and Lipid Synthesis, Trends Endocrinol Metab, 27 (2016) 719–730. [PubMed: 27387598]

[30]. Zhang D, Tong X, VanDommelen K, Gupta N, Stamper K, Brady GF, Meng Z, Lin J, Rui L, Omary MB, Yin L, Lipogenic transcription factor ChREBP mediates fructose-induced metabolic adaptations to prevent hepatotoxicity, J CLIN INVEST, 127 (2017) 2855–2867. [PubMed: 28628040]

[31]. Koo HY, Wallig MA, Chung BH, Nara TY, Cho BH, Nakamura MT, Dietary fructose induces a wide range of genes with distinct shift in carbohydrate and lipid metabolism in fed and fasted rat liver, Biochim Biophys Acta, 1782 (2008) 341–348. [PubMed: 18346472]

[32]. Makinen VP, Civelek M, Meng Q, Zhang B, Zhu J, Levian C, Huan T, Segre AV, Ghosh S, Vivar J, Nikpay M, Stewart AF, Nelson CP, Willenborg C, Erdmann J, Blakenberg S, O'Donnell CJ, Marz W, Laaksonen R, Epstein SE, Kathiresan S, Shah SH, Hazen SL, Reilly MP, Coronary ADG-WR, Meta-Analysis C, Lusis AJ, Samani NJ, Schunkert H, Quertermous T, McPherson R, Yang X, Assimes TL, Integrative genomics reveals novel molecular pathways and gene networks for coronary artery disease, PLOS GENET, 10 (2014) e1004502. [PubMed: 25033284]

[33]. Shu L, Chan KHK, Zhang G, Huan T, Kurt Z, Zhao Y, Codoni V, Tregouet DA, Cardiogenics C, Yang J, Wilson JG, Luo X, Levy D, Lusis AJ, Liu S, Yang X, Shared genetic regulatory networks for cardiovascular disease and type 2 diabetes in multiple populations of diverse ethnicities in the United States, PLOS GENET, 13 (2017) e1007040. [PubMed: 28957322]

[34]. Chella Krishnan K, Kurt Z, Barrere-Cain R, Sabir S, Das A, Floyd R, Vergnes L, Zhao Y, Che N, Charugundla S, Qi H, Zhou Z, Meng Y, Pan C, Seldin MM, Norheim F, Hui S, Reue K, Lusis AJ, Yang X, Integration of Multi-omics Data from Mouse Diversity Panel Highlights Mitochondrial Dysfunction in Non-alcoholic Fatty Liver Disease, CELL SYST, 6 (2018) 103–115 e107. [PubMed: 29361464]

[35]. Xu J, Stanislaus S, Chinookoswong N, Lau YY, Hager T, Patel J, Ge H, Weiszmann J, Lu SC, Graham M, Busby J, Hecht R, Li YS, Li Y, Lindberg R, Veniant MM, Acute glucose-lowering and insulin-sensitizing action of FGF21 in insulin-resistant mouse models--association with liver and adipose tissue effects, Am J Physiol Endocrinol Metab, 297 (2009) E1105–1114. [PubMed: 19706786]

[36]. Le Martelot G, Claudel T, Gatfield D, Schaad O, Kornmann B, Lo Sasso G, Moschetta A, Schibler U, REV-ERBalpha participates in circadian SREBP signaling and bile acid homeostasis, PLOS BIOL, 7 (2009) e1000181. [PubMed: 19721697]

[37]. Schmidt EA, Fee BE, Henry SC, Nichols AG, Shinohara ML, Rathmell JC, MacIver NJ, Coers J, Ilkayeva OR, Koves TR, Taylor GA, Metabolic Alterations Contribute to Enhanced Inflammatory Cytokine Production in Irgm1-deficient Macrophages, J BIOL CHEM, 292 (2017) 4651–4662. [PubMed: 28154172]

[38]. Wickramasekara RN, Morrill S, Farhat Y, Smith SJ, Yilmazer-Hanke D, Glutathione and Inter-alpha-trypsin inhibitor heavy chain 3 (Itih3) mRNA levels in nicotine-treated Cd44 knockout mice, Toxicol Rep, 5 (2018) 759–764. [PubMed: 29984189]

[39]. Drury JE, Mindnich R, Penning TM, Characterization of disease-related 5beta-reductase (AKR1D1) mutations reveals their potential to cause bile acid deficiency, J BIOL CHEM, 285 (2010) 24529–24537. [PubMed: 20522910]

[40]. Favennec M, Hennart B, Caiazzo R, Leloire A, Yengo L, Verbanck M, Arredouani A,Marre M, Pigeyre M, Bessede A, Guillemin GJ, Chinetti G, Staels B, Pattou F, Balkau B, Allorge D, Froguel P, Poulain-Godefroy O, The kynurenine pathway is activated in human obesity and shifted toward kynurenine monooxygenase activation, Obesity (Silver Spring), 23 (2015) 2066–2074. [PubMed: 26347385]

[41]. Ying Z, Byun HR, Meng Q, Noble E, Zhang G, Yang X, Gomez-Pinilla F, Biglycan gene connects metabolic dysfunction with brain disorder, Biochim Biophys Acta Mol Basis Dis, 1864 (2018) 3679–3687. [PubMed: 30291886]

[42]. Shu L, Zhao Y, Kurt Z, Byars SG, Tukiainen T, Kettunen J, Orozco LD, Pellegrini M, Lusis AJ, Ripatti S, Zhang B, Inouye M, Makinen VP, Yang X, Mergeomics: multidimensional data integration to identify pathogenic perturbations to biological systems, BMC GENOMICS, 17 (2016) 874. [PubMed: 27814671]

[43]. Nakayama K, Bayasgalan T, Tazoe F, Yanagisawa Y, Gotoh T, Yamanaka K, Ogawa A, Munkhtulga L, Chimedregze U, Kagawa Y, Ishibashi S, Iwamoto S, Jichi J Medical University Promotion Team of a Large-scale Human Genome Bank for All over, A single nucleotide polymorphism in the FADS1/FADS2 gene is associated with plasma lipid profiles in two genetically similar Asian ethnic groups with distinctive differences in lifestyle, HUM GENET, 127 (2010) 685–690. [PubMed: 20364269]

[44]. Yin RX, Wu DF, Miao L, Aung LH, Cao XL, Yan TT, Long XJ, Liu WY, Zhang L, Li M, Several genetic polymorphisms interact with overweight/obesity to influence serum lipid levels, CARDIOVASC DIABETOL, 11 (2012) 123. [PubMed: 23039238]

[45]. Nie L, Wang J, Clark LT, Tang A, Vega GL, Grundy SM, Cohen JC, Body mass index and hepatic lipase gene (LIPC) polymorphism jointly influence postheparin plasma hepatic lipase activity, J LIPID RES, 39 (1998) 1127–1130. [PubMed: 9610782]

[46]. Zeevi D, Korem T, Zmora N, Israeli D, Rothschild D, Weinberger A, Ben-Yacov O, Lador D, Avnit-Sagi T, Lotan-Pompan M, Suez J, Mahdi JA, Matot E, Malka G, Kosower N, Rein M, Zilberman-Schapira G, Dohnalova L, Pevsner-Fischer M, Bikovsky R, Halpern Z, Elinav E, Segal E, Personalized Nutrition by Prediction of Glycemic Responses, CELL, 163 (2015) 1079–1094. [PubMed: 26590418]

[47]. Jimenez V, Jambrina C, Casana E, Sacristan V, Munoz S, Darriba S, Rodo J, Mallol C, Garcia M, Leon X, Marco S, Ribera A, Elias I, Casellas A, Grass I, Elias G, Ferre T, Motas S, Franckhauser S, Mulero F, Navarro M, Haurigot V, Ruberte J, Bosch F, FGF21 gene therapy as treatment for obesity and insulin resistance, EMBO MOL MED, 10 (2018).

[48]. Li H, Wu G, Fang Q, Zhang M, Hui X, Sheng B, Wu L, Bao Y, Li P, Xu A, Jia W, Fibroblast growth factor 21 increases insulin sensitivity through specific expansion of subcutaneous fat, NAT COMMUN, 9 (2018) 272. [PubMed: 29348470]

[49]. Karunagaran S, Kavitha R, Vadivelu M, Lee KW, Meganathan C, Insight Mechanism of the Selective Lanosterol Synthase Inhibitor: Molecular Modeling, Docking and Density Functional Theory Approaches, Curr Comput Aided Drug Des, 13 (2017) 275–293. [PubMed: 28462697]

[50]. Le KA, Ith M, Kreis R, Faeh D, Bortolotti M, Tran C, Boesch C, Tappy L, Fructose overconsumption causes dyslipidemia and ectopic lipid deposition in healthy subjects with and without a family history of type 2 diabetes, AM J CLIN NUTR, 89 (2009) 1760–1765. [PubMed: 19403641]

[51]. Beck-Nielsen H, Pedersen O, Lindskov HO, Impaired cellular insulin binding and insulin sensitivity induced by high-fructose feeding in normal subjects, AM J CLIN NUTR, 33 (1980) 273–278. [PubMed: 6986758]

[52]. Choo VL, Viguiliouk E, Blanco Mejia S, Cozma AI, Khan TA, Ha V, Wolever TMS, Leiter LA, Vuksan V, Kendall CWC, de Souza RJ, Jenkins DJA, Sievenpiper JL, Food sources of fructose-containing sugars and glycaemic control: systematic review and meta-analysis of controlled intervention studies, BMJ, 363 (2018) k4644. [PubMed: 30463844]

[53]. Alegret M, Roglans N, Laguna J, Fructose consumption and leptin resistance: What have we learnt from animal studies?, in, 2011, pp. 209–230.

[54]. Hokayem M, Blond E, Vidal H, Lambert K, Meugnier E, Feillet-Coudray C, Coudray C, Pesenti S, Luyton C, Lambert-Porcheron S, Sauvinet V, Fedou C, Brun JF, Rieusset J, Bisbal C, Sultan A, Mercier J, Goudable J, Dupuy AM, Cristol JP, Laville M, Avignon A, Grape polyphenols prevent fructose-induced oxidative stress and insulin resistance in first-degree relatives of type 2 diabetic patients, DIABETES CARE, 36 (2013) 1454–1461. [PubMed: 23275372]

[55]. Seyssel K, Meugnier E, Le KA, Durand C, Disse E, Blond E, Pays L, Nataf S, Brozek J, Vidal H, Tappy L, Laville M, Fructose overfeeding in first-degree relatives of type 2 diabetic patients impacts energy metabolism and mitochondrial functions in skeletal muscle, MOL NUTR FOOD RES, 60 (2016) 2691–2699. [PubMed: 27468128]

[56]. Bahar Halpern K, Tanami S, Landen S, Chapal M, Szlak L, Hutzler A, Nizhberg A, Itzkovitz S, Bursty gene expression in the intact mammalian liver, MOL CELL, 58 (2015) 147–156. [PubMed: 25728770]

[57]. Haas JT, Miao J, Chanda D, Wang Y, Zhao E, Haas ME, Hirschey M, Vaitheesvaran B, Farese RV Jr., Kurland IJ, Graham M, Crooke R, Foufelle F, Biddinger SB, Hepatic insulin signaling is required for obesity-dependent expression of SREBP-1c mRNA but not for feeding-dependent expression, CELL METAB, 15 (2012) 873–884. [PubMed: 22682225]

[58]. Linden AG, Li S, Choi HY, Fang F, Fukasawa M, Uyeda K, Hammer RE, Horton JD, Engelking LJ, Liang G, Interplay between ChREBP and SREBP-1c coordinates postprandial glycolysis and lipogenesis in livers of mice, J LIPID RES, 59 (2018) 475–487. [PubMed: 29335275]

[59]. Madigan D, York J, Bayesian Graphical Models for Discrete-Data, INT STAT REV, 63 (1995) 215–232.

[60]. Zhu J, Lum PY, Lamb J, GuhaThakurta D, Edwards SW, Thieringer R, Berger JP, Wu MS, Thompson J, Sachs AB, Schadt EE, An integrative genomics approach to the reconstruction of gene networks in segregating populations, CYTOGENET GENOME RES, 105 (2004) 363–374. [PubMed: 15237224]

Highlights

- Fructose induced strain-specific metabolic responses in genetically distinct mice.
- Fructose altered strain-specific transcriptome in liver, adipose, and hypothalamus.
- Fructose altered strain- and tissue-specific genes, pathways, and networks.
- Strain- and tissue-specific regulatory genes were identified and validated in vitro.
- Fructose-responsive genes were associated with metabolic traits in mice and human.

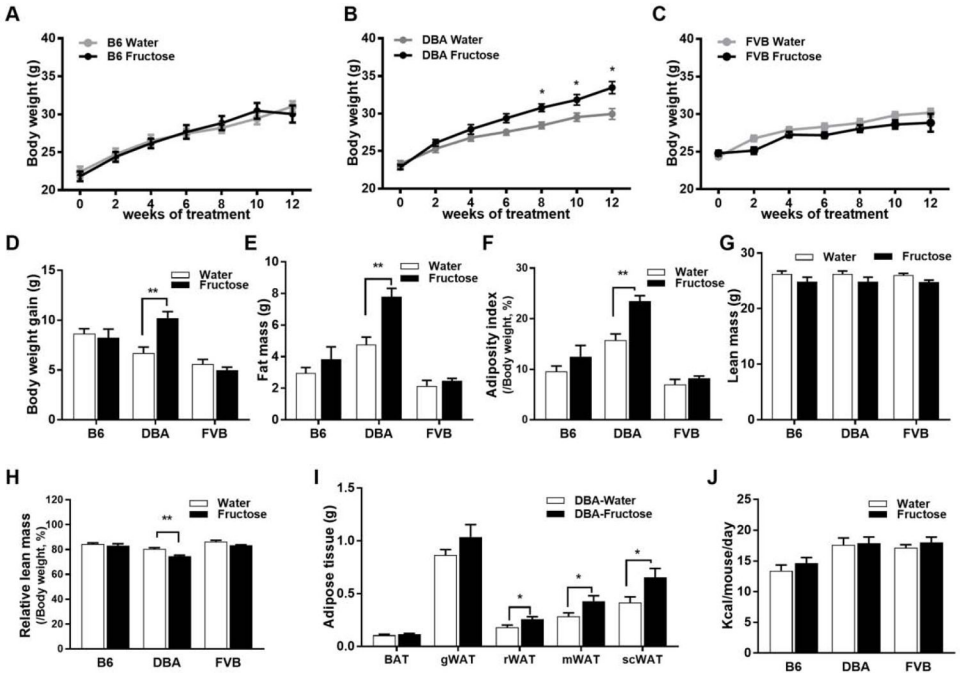

Fig. 1. Body weight and body composition changes and caloric intake in three strains of mice in response to fructose consumption.

A–C: Cumulative change in body weight in B6 (A), DBA (B) and FVB (C) mice fed normal Chow diet with water or 8% fructose over 12 weeks. Two-way ANNOVA was used to test the differences between treatment groups and time points, followed by Sidak post-hoc analysis to examine treatment effects at individual time points. * denotes $P < 0.05$ from the post-hoc analysis. D: body weight gain at the end of experiment. E-H: Body composition change in three strains of mice, with fat mass (E), percent fat mas (F), lean mass (G), percent lean mass (H) measured using NMR. I: Individual fat masses of DBA mice. BAT: brown adipose tissue; gWAT: gonadal white adipose tissue; rWAT: retroperitoneal white adipose tissue; mWAT: mesenteric white adipose tissue; scWAT: subcutaneous white adipose tissue. J: Caloric intake of three stains of mice. Error bars in the graph are standard errors. E-K: * denotes $P < 0.05$ and ** denotes $P < 0.01$ by two-sided Student's t-test. Sample size n=8–12/group/strain.

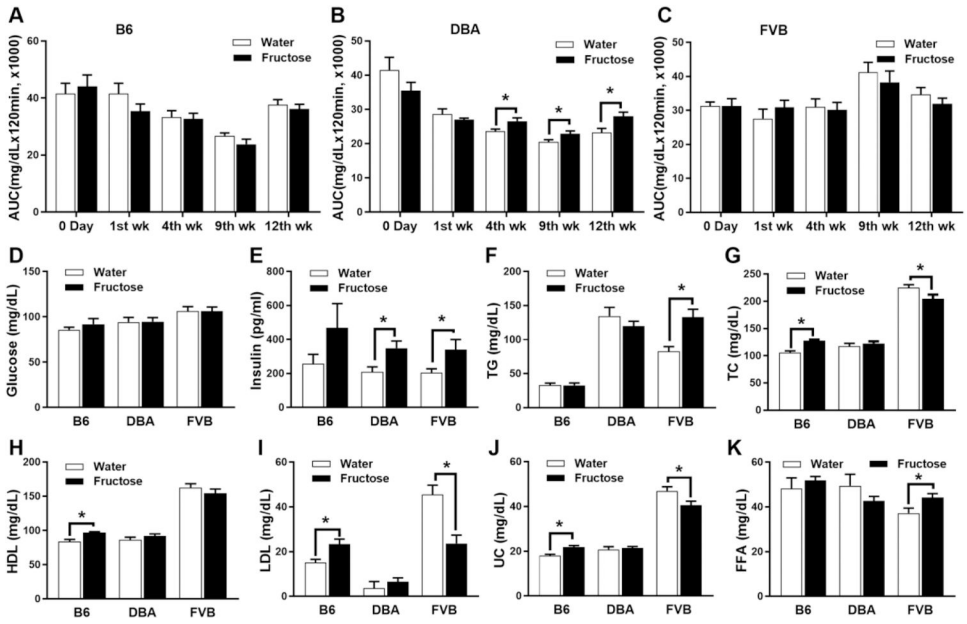

Fig. 2. Glucose metabolism and lipid changes in three strains of mice in response to fructose consumption.

A–C: Glucose tolerance analysis using IPGTT were conducted at baseline (0 day), 1st, 4th, 9th and 12th week shown as area under the curve (AUC). D: Plasma glucose. E: Plasma insulin. F: Plasma triglyceride. G: Plasma total cholesterol. H: HDL. I: LDL. J: Unesterified cholesterol. K: Free fatty acid levels. A–K: sample size n=8–10 per group. $*P < 0.05$ and $**P < 0.01$ by two-sided Student's t-test.

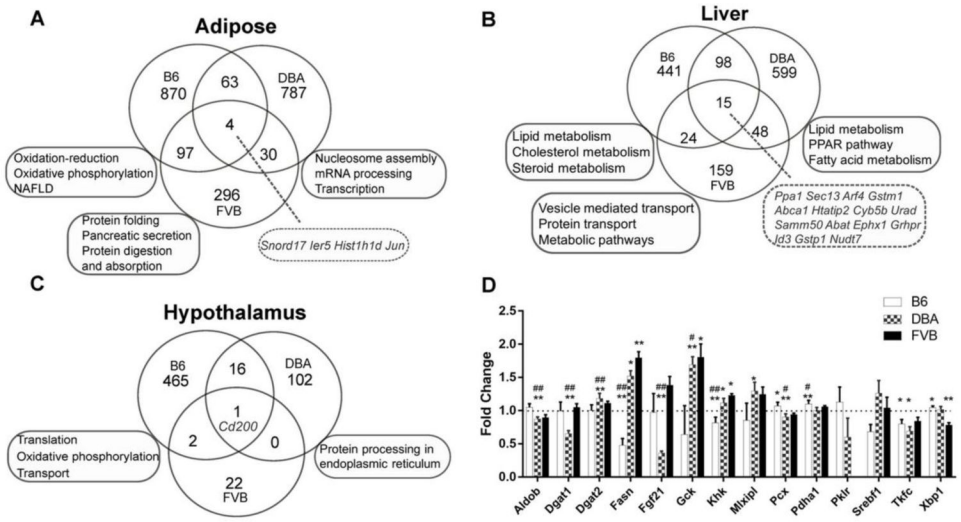

Fig. 3. Differentially expressed genes (DEGs) and representative over-represented pathways in adipose, liver and hypothalamus of three mouse strains.

A–C: Venn diagrams of adipose (A), liver (B), and hypothalamus (C) DEGs and pathways across three strains. D: Fold change and significance of gene expression differences between fructose and control groups for known target genes of fructose, ChREBP (encoded by *Mlxipl*), SREBP-1c (encoded by *Srebf1*) in the three mouse strains. Fold change for each gene is the normalized average expression level in fructose mice over that of the control mice. * $P < 0.05$, ** $P < 0.01$, # FDR<5%, ## FDR<1% in RNAseq analysis using a linear model. Sample size n=6/group/tissue/strain for liver; n=3–6/group/tissue/strain for adipose tissues; n=4/group/strain for hypothalamus tissue.

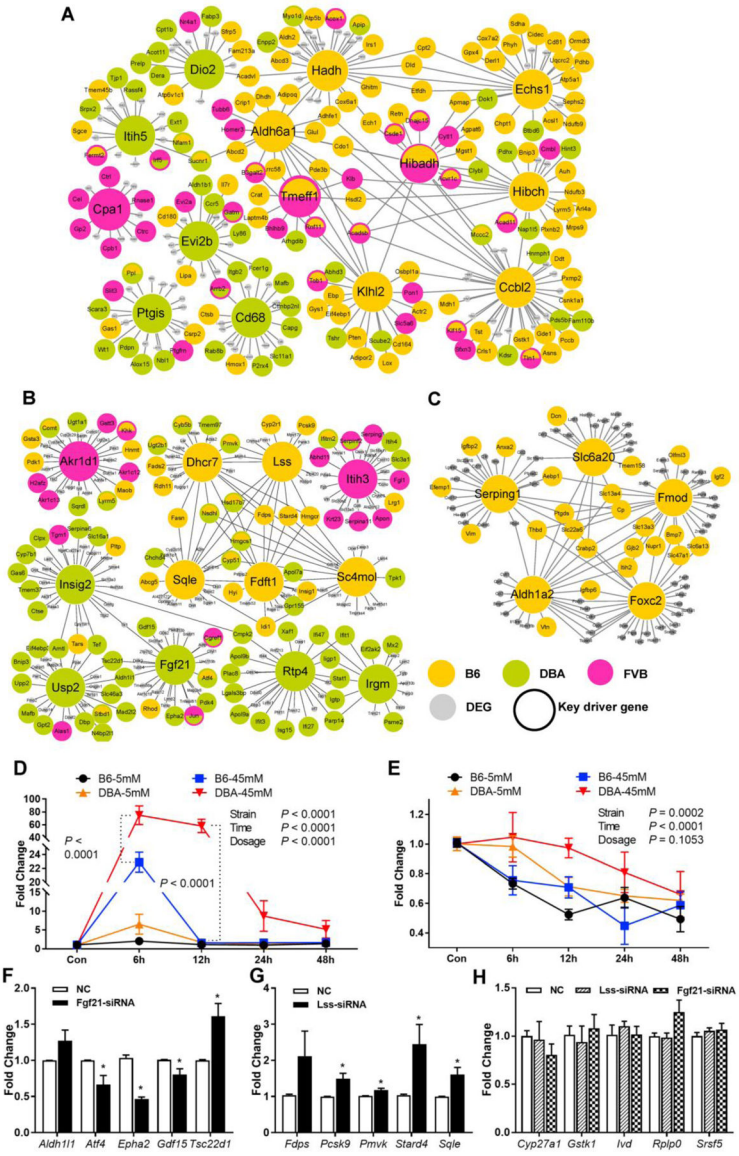

Fig. 4. Gene subnetworks and top network key drivers (KDs) of DEGs in three strains of mice and validation of select strain-specific liver KDs in primary hepatocytes.

A: Top adipose KDs and subnetworks. B: Top liver KDs and subnetworks. C: Top hypothalamus KDs and subnetworks. D: Direct response to fructose for DBA-specific KD *Fgf21* is stronger in DBA hepatocytes than in B6 hepatocytes. E: Direct response to fructose for B6-specific KD *Lss* is stronger in B6 hepatocytes than in DBA hepatocytes. D–E: P values for strain, fructose concentration, and time points are from 3-way ANOVA. At each concentration and time point, p values between mouse strains are from Tukey post-hoc analysis. Sample size n=3 (2 replicates/mice) per strain per concentration per time point. F: Expression changes of genes in *Fgf21*-driven network after siRNA-mediated knockdown of *Fgf21* in DBA primary hepatocytes. Genes surrounding *Fgf21* were selected from Fig. 4B. G: Expression changes of genes in *Lss*-driven network after siRNA-mediated knockdown of *Lss* in B6 primary hepatocytes. Genes surrounding *Lss* were selected from Fig. 4B. H: Gene expression of DEGs not shown in *Fgf21/Lss* gene networks (negative controls). F-H: NC

represents scrambled siRNAs as negative controls. *$P < 0.05$ and **$P < 0.01$ by two-sided Student's t-test. Sample size n=3 (2 replicates/siRNA).

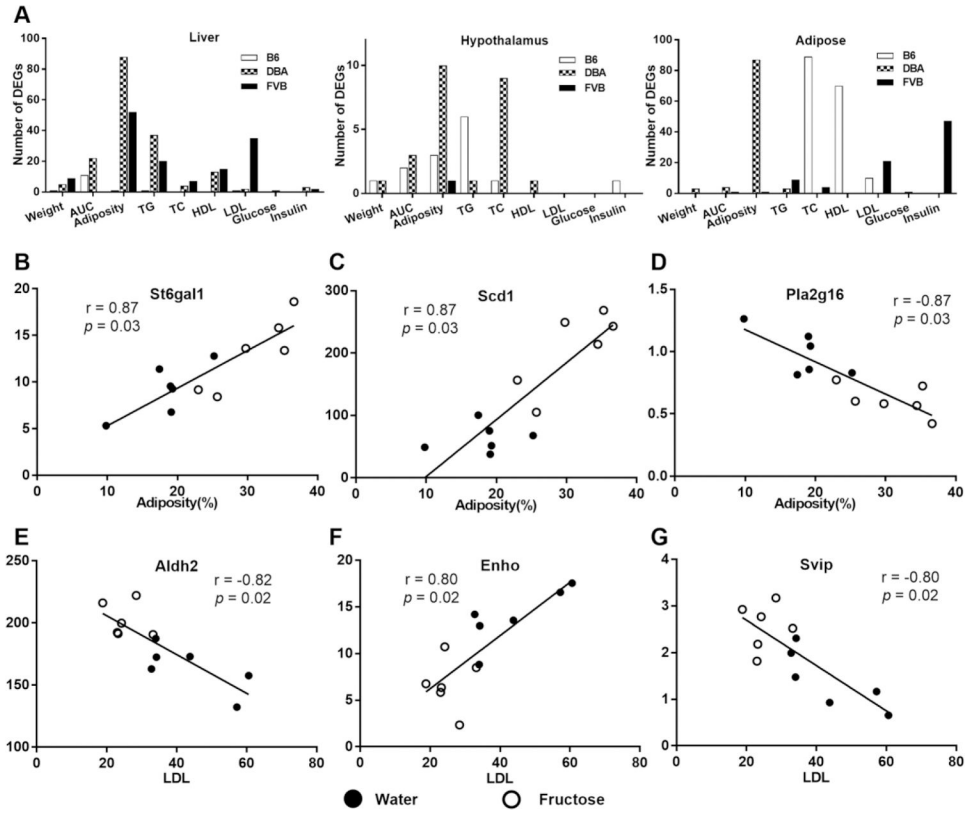

Fig. 5. Relationship between DEGs and metabolic traits in mice.

A: Numbers of strain-specific DEGs that are correlated with metabolic traits in our fructose study ($P < 0.01$ by Pearson correlation). B–D: Select examples of DEGs in liver correlating with adiposity in DBA mice. E–G: Select examples of DEGs in liver correlating with LDL in FVB mice.

Table 1.

Summary of DEGs in liver, adipose and hypothalamus tissues of three mouse strains at FDR< 0.05 and their top representative key drivers (KDs).

Full lists of DEGs, pathways, and KDs are in Supplementary Tables 3–5.

Tissue	Strain	DEG No.	Top over-represented pathways	Top representative KDs
Liver	B6	578	Oxidation-reduction process, Metabolic pathways, Lipid metabolic process, Biosynthesis of antibiotics, Cholesterol metabolic process	*Dhcr7, Fdft1, Lss, Sc4mol, Sqle*
	DBA	760	Oxidation-reduction process, Metabolic pathways, Lipid metabolic process, PPAR signaling pathway, Fatty acid metabolic process	*Rtp4, Usp2, Irgm, Insig2, Fgf21*
	FVB	246	Vesicle-mediated transport, protein transport, Metabolic pathways, oxidation-reduction process, Chemical carcinogenesis	*Itih3, Akr1d1*
Adipose	B6	1034	Oxidation reduction process, TCA cycle and respiratory electron transport, Non-alcoholic fatty liver disease (NAFLD), Lipid metabolic pathways	*Aldh6a1, Echs1, Hadh, Hibadh, Hibch*
	DBA	884	Nucleosome assembly	*Evi2b, Cd68, Dio2, Itih5, Ptgis*
	FVB	427	Protein folding, Response to topologically incorrect protein, Protein complex subunit organization, Cellular component disassembly, Catabolic process	*Klhl2, Ccbl2, Hibch, Tmeff1, Cpa1*
Hypothalamus	B6	484	Ribosome, Translation, Transport, Oxidative phosphorylation, Mitochondrial respiratory chain complex III assembly	*Fmod, Gpr81, Aldh1a2, Serping1, Slc22a6, Bgn*
	DBA	119	Protein processing in endoplasmic reticulum, Response to endoplasmic reticulum stress	None
	FVB	25	None	None

Table 2.

Enrichment of human GWAS signals for metabolic syndrome related traits among strain- and tissue-specific DEGs based on Marker Set Enrichment Analysis (MSEA) in Mergeomics.

Tissue of DEGs	Disease/trait	B6	DBA	FVB
Liver	CAD	**9.65E-05**	N.S	**2.85E-31**
	T2D	**6.56E-08**	**4.02E-08**	N.S
	HDL	**3.30E-05**	N.S	**8.90E-15**
	LDL	2.96E-03	**3.77E-05**	N.S
	TC	N.S	2.57E-02	3.51E-03
	TG	**7.43E-12**	1.93E-03	1.24E-03
	Fasting glucose	N.S	**4.60E-04**	1.30E-03
	WCadjBMI	N.S	N.S	1.54E-03
	HIPadjBMI	**2.37E-06**	**2.06E-09**	2.77E-03
Adipose	T2D	**1.72E-13**	N.S	N.S
	HDL	**8.80E-41**	**1.25E-07**	4.10E-02
	LDL	N.S	N.S	**8.09E-18**
	TC	**9.41E-07**	N.S	N.S
	TG	**1.87E-12**	3.53E-03	**8.12E-07**
	Obesity	**4.89E-05**	**2.34E-10**	N.S
	WCadjBMI	**3.58E-36**	N.S	**5.17E-07**
	HIPadjBMI	**8.81E-23**	N.S	**1.17E-07**
Hypothalamus	HDL	1.57E-02	N.S	N.S
	LDL	1.57E-02	N.S	N.S
	TC	9.64E-03	N.S	N.S
	TG	2.36E-02	N.S	N.S
	Obesity	2.41E-02	N.S	N.S

Note: Only traits and statistics with uncorrected MSEA enrichment $P < 0.05$ from at least one DEG list were shown. P values in bold passed Bonferroni-corrected $P < 0.05$. CAD: coronary artery disease; T2D: type 2 diabetes; HDL: high density lipoprotein cholesterol; LDL: low density lipoprotein cholesterol; TC: total cholesterol; TG: triglycerides; WCadjBMI: BMI-adjusted waist circumference; HIPadjBMI: BMI-adjusted hip circumference. N.S.: not significant; $P > 0.05$ in MSEA.